Enantiomeric Separation of Semiconducting Single-Walled Carbon Nanotubes by Acid Cleavable Chiral Polyfluorene

Liang Xu, Michal Valášek,* Frank Hennrich, Elaheh Sedghamiz, Montserrat Penaloza-Amion, Daniel Häussinger, Wolfgang Wenzel, Manfred M. Kappes,* and Marcel Mayor*

ABSTRACT: Helical wrapping by conjugated polymer has been demonstrated as a powerful tool for the sorting of single walled carbon nanotubes (SWCNTs) according to their electronic type, chiral index, and even handedness. However, a method of one step extraction of left handed (*M*) and right handed (*P*) semiconducting SWCNTs (s SWCNTs) with subsequent cleavage of the polymer has not yet been published. In this work, we designed and synthesized one pair of acid cleavable polyfluorenes with defined chirality for handedness separation of s SWCNTs from as produced nanotubes. Each monomer contains a chiral center on the fluorene backbone in the 9 position, and the amino and carbonyl groups in the 2 and 7 positions maintain the head to tail regioselective polymerization resulting in polyimines with strictly all (*R*) or all (*S*) configuration. The obtained chiral polymers exhibit a strong recognition ability toward left or right handed s SWCNTs from commercially available CoMoCAT SWCNTs with a sorting process requiring only bath sonication and centrifugation. Interestingly, the remaining polymer on each single nanotube, which helps to prevent aggregation, does not interfere with the circular dichroism signals from the nanotube at all. Therefore, we observed all four interband transition peaks (E_{11}, E_{22}, E_{33}, E_{44}) in the circular dichroism (CD) spectra of the still wrapped optically enriched left handed and right handed (6,5) SWCNTs in toluene. Binding energies obtained from molecular dynamics simulations were consistent with our experimental results and showed a significant preference for one specific handedness from each chiral polymer. Moreover, the imine bonds along the polymer chains enable the release of the nanotubes upon acid treatment. After s SWNT separation, the polymer can be decomposed into monomers and be cleanly removed under mild acidic conditions, yielding dispersant free handedness sorted s SWNTs. The monomers can be almost quantitatively recovered to resynthesize the chiral polymer. This approach enables high selective isolation of polymer free s SWNT enantiomers for their further applications in carbon nanotube (CNT) devices.

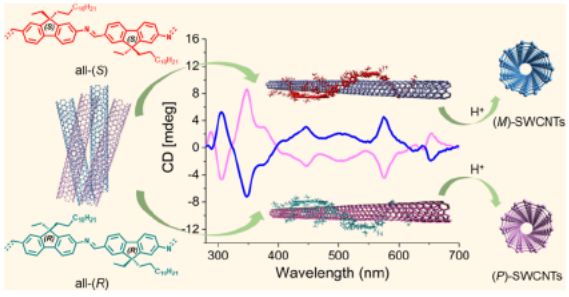

KEYWORDS: *SWCNT, enantiomeric separation, handedness, conjugated polymer, chiral polyfluorene, circular dichroism, molecular dynamics*

Single walled carbon nanotubes (SWCNTs) are among the most intensively studied nanomaterials since their discovery in the 1990s,[1] owing to their extraordinary physical, electronic, and optical properties.[2−6] For their diverse applications as field effect transistors (FETs),[7−9] thin films,[10−12] and optoelectronics[13,14] and for computing,[15] highly enriched SWCNTs with a specific conductivity (metallic or semi conducting) and chiral index (*n*,*m*) are of great importance. Bottom up organic synthesis has always been considered promising toward tailor made SWCNTs; however, a scalable method for controlled growth on precursors and template molecules is still under investigation.[16−18] An alternative approach for the enrichment of desired SWCNTs is to sort them in solution from the as produced carbon nanotube (CNT) mixture, such as HiPco and CoMoCAT tubes. Various scalable methods have been developed to achieve chiral index pure SWCNTs in solution.[19−25]

Nevertheless, the resulting single chiral index SWCNTs are actually racemic mixtures of two enantiomers, namely, left handed and right handed isomers. Enantiomerically pure

After simple sonication and centrifugation steps, the chiral polymers showed high selectivity toward s SWCNTs and spontaneously recognized left handed and right handed nano tubes according to their preference. The imine bonds enable the easy removal of the polymer from the nanotubes and the subsequent redispersion of the released nanotube enantiomers with other dispersants. Additionally, the building blocks after depolymerization can almost quantitatively be recycled and reused for the synthesis of the polymers. In order to understand the origin of the selective interaction between the chiral polymers and s SWCNTs, molecular dynamics (MD) simu lations in explicit solvent have been conducted, showing a high preference of one specific nanotube handedness with a certain wrapping direction from each chiral polymer.

RESULTS AND DISCUSSION

Synthesis and Characterization of Enantiomeric Monomers and Polymers. The racemic monomer **1** (Figure 2) was synthesized in five steps starting from 2,7 dibromo

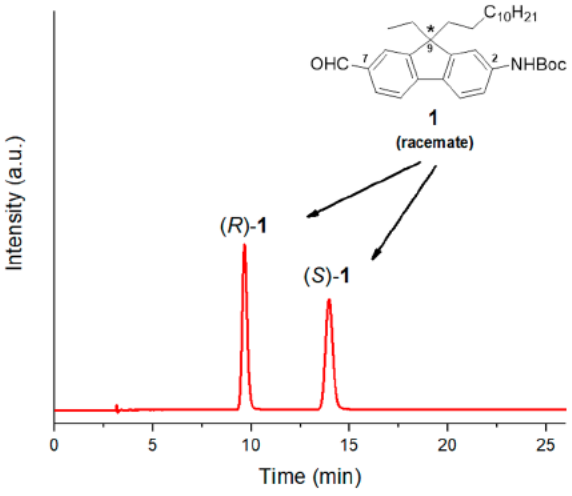

Figure 2. Chiral HPLC chromatogram of racemic monomer 1 (*n* heptane/IPA = 96:4). The inset structure of 1 shows the corresponding numbering.

fluorene (see the Supporting Information, Experimental details and synthetic procedures). The subsequent preparative resolution of two Boc protected enantiomers of **1** was achieved using chiral HPLC as shown in Figure 2.

The determination of the absolute configuration of both enantiomeric monomers (*R*) **1** and (*S*) **1** was carried out by Mosher's ester method.[44,45] All details about the synthesis of the Mosher derivatives of **1** and their NMR analyses are given in the Supporting Information. The 2D NMR analysis revealed that the first enantiomer eluted at $R_t \sim 10$ min has an (*R*) configuration while the second one eluted at $R_t \sim 14$ min has an (*S*) configuration. After removal of the amine protecting Boc group of **1** under acidic conditions, we found out that the unprotected monomers spontaneously polymerized to the corresponding polyimines even during the workup in rather mild conditions. Therefore, after the workup and removal of the solvent, deprotected (*R*) **1**, (*S*) **1**, and racemic **1** monomers were *in situ* neat polymerized at 100 °C under reduced pressure without any solvent or catalyst to afford the corresponding chiral polymers (*R*) CP, (*S*) CP, and achiral polymer ACP in nearly quantitative yields, respectively (Figure 1 and Supporting Information). Due to the quick polymerization under mild conditions and the molecular design of monomers for head to tail polymerization with a stable quaternary stereocenter at the 9 position of the fluorene unit, the obtained (*R*) CP and (*S*) CP polymers maintained all (*R*) and all (*S*) configurations, respectively. The gel permeation chromatography (GPC) results (Figure 3) show that all three polymers have a broad

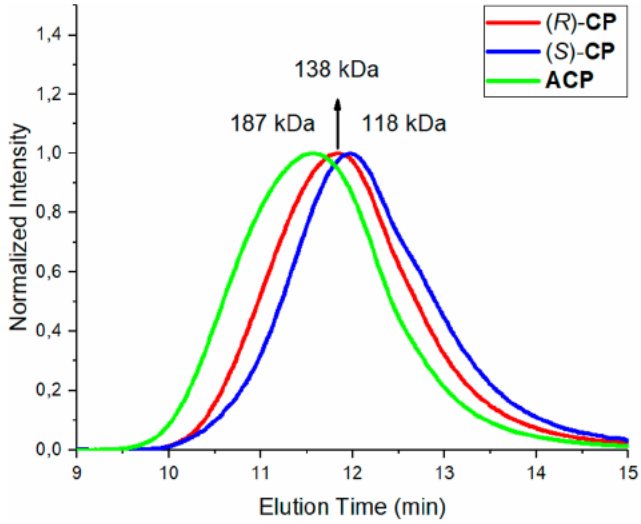

Figure 3. GPC results of (R) CP, (S) CP, and ACP with peak molecular weights of 138 kDa ($n \sim 356$), 118 kDa ($n \sim 304$), and 187 kDa ($n \sim 482$), respectively. All samples were measured with a concentration of 1 mg/mL in THF at 25 °C.

distribution of molecular weight over 118 kDa ($n > 300$), referred to the polystyrene molecular weight standards. The comparable molecular weights of both chiral polymers benefit the evaluation and comparison of their enantiomeric recognition ability. This synthetic procedure for the chiral polymers is fully reproducible.

In order to prove that both polyimines (*R*) CP and (*S*) CP as well as the monomers (*R*) **1** and (*S*) **1** are chiral and optically active, circular dichroism (CD) absorbance spectroscopy measurements were carried out in toluene at 25 °C (Figure 4a,b). The CD spectra of these enantiomers are mirror images of one another, confirming their enantiopurity.

Surprisingly, it has been shown that CD spectra of both monomers and polymers exhibit quite weak and noisy signals even with the concentration up to 10^{-4} M. Chirality of the monomers **1** originates from the presence of asymmetric sp^3 carbon at the 9 position of the fluorene chromophore bearing two nonpolar alkyl chains that differ only in the chain length (ethyl vs dodecyl). Additionally, the other two substituents that are in positions 2 and 7 of the fluorene unit are far away from the chiral sp^3 center and thus contribute very little to the overall chirality of the monomers. Therefore, this minor substitution effect together with the rigidity of the fluorene structure and the steric hindrance of the chiral C9 center lead to the low response of the chiral monomers to circularly polarized light. To further interpret the observed CD spectra of the monomers, the time dependent (TD) DFT calculations were used to simulate the absorption and CD spectra and to determine the transitions in the spectra (see the Supporting Information). The observed CD peak in the experimental spectra of the monomers at ~310 nm (Figure 4a) corresponds to the minor peak in the calculated CD spectra, which can be attributed to the HOMO → LUMO+1 transition (Figure S33).

After simple sonication and centrifugation steps, the chiral polymers showed high selectivity toward s SWCNTs and spontaneously recognized left handed and right handed nano tubes according to their preference. The imine bonds enable the easy removal of the polymer from the nanotubes and the subsequent redispersion of the released nanotube enantiomers with other dispersants. Additionally, the building blocks after depolymerization can almost quantitatively be recycled and reused for the synthesis of the polymers. In order to understand the origin of the selective interaction between the chiral polymers and s SWCNTs, molecular dynamics (MD) simu lations in explicit solvent have been conducted, showing a high preference of one specific nanotube handedness with a certain wrapping direction from each chiral polymer.

RESULTS AND DISCUSSION

Synthesis and Characterization of Enantiomeric Monomers and Polymers. The racemic monomer **1** (Figure 2) was synthesized in five steps starting from 2,7 dibromo

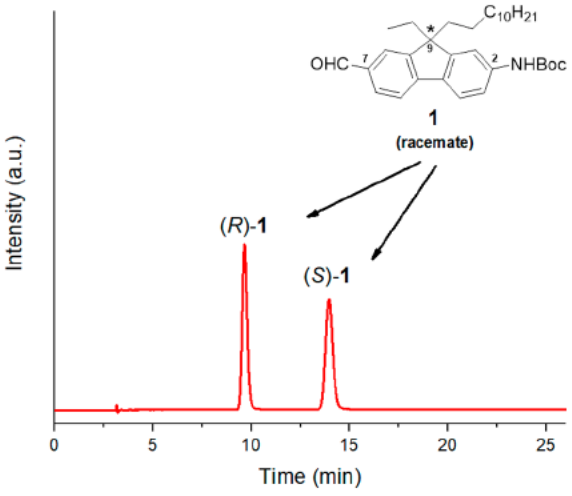

Figure 2. Chiral HPLC chromatogram of racemic monomer 1 (*n* heptane/IPA = 96:4). The inset structure of 1 shows the corresponding numbering.

fluorene (see the Supporting Information, Experimental details and synthetic procedures). The subsequent preparative resolution of two Boc protected enantiomers of **1** was achieved using chiral HPLC as shown in Figure 2.

The determination of the absolute configuration of both enantiomeric monomers (*R*) **1** and (*S*) **1** was carried out by Mosher's ester method.[44,45] All details about the synthesis of the Mosher derivatives of **1** and their NMR analyses are given in the Supporting Information. The 2D NMR analysis revealed that the first enantiomer eluted at $R_t \sim 10$ min has an (*R*) configuration while the second one eluted at $R_t \sim 14$ min has an (*S*) configuration. After removal of the amine protecting Boc group of **1** under acidic conditions, we found out that the unprotected monomers spontaneously polymerized to the corresponding polyimines even during the workup in rather mild conditions. Therefore, after the workup and removal of the solvent, deprotected (*R*) **1**, (*S*) **1**, and racemic **1** monomers were *in situ* neat polymerized at 100 °C under reduced pressure without any solvent or catalyst to afford the corresponding chiral polymers (*R*) CP, (*S*) CP, and achiral polymer ACP in nearly quantitative yields, respectively (Figure 1 and Supporting Information). Due to the quick polymerization under mild conditions and the molecular design of monomers for head to tail polymerization with a stable quaternary stereocenter at the 9 position of the fluorene unit, the obtained (*R*) CP and (*S*) CP polymers maintained all (*R*) and all (*S*) configurations, respectively. The gel permeation chromatography (GPC) results (Figure 3) show that all three polymers have a broad

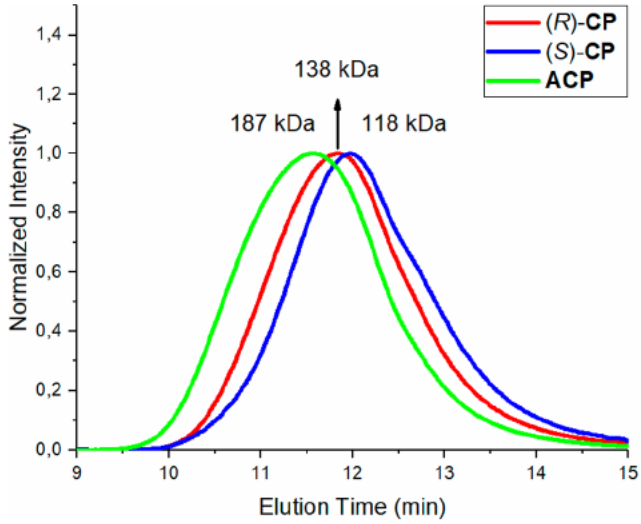

Figure 3. GPC results of (R) CP, (S) CP, and ACP with peak molecular weights of 138 kDa ($n \sim 356$), 118 kDa ($n \sim 304$), and 187 kDa ($n \sim 482$), respectively. All samples were measured with a concentration of 1 mg/mL in THF at 25 °C.

distribution of molecular weight over 118 kDa ($n > 300$), referred to the polystyrene molecular weight standards. The comparable molecular weights of both chiral polymers benefit the evaluation and comparison of their enantiomeric recognition ability. This synthetic procedure for the chiral polymers is fully reproducible.

In order to prove that both polyimines (*R*) CP and (*S*) CP as well as the monomers (*R*) **1** and (*S*) **1** are chiral and optically active, circular dichroism (CD) absorbance spectroscopy measurements were carried out in toluene at 25 °C (Figure 4a,b). The CD spectra of these enantiomers are mirror images of one another, confirming their enantiopurity.

Surprisingly, it has been shown that CD spectra of both monomers and polymers exhibit quite weak and noisy signals even with the concentration up to 10^{-4} M. Chirality of the monomers **1** originates from the presence of asymmetric sp^3 carbon at the 9 position of the fluorene chromophore bearing two nonpolar alkyl chains that differ only in the chain length (ethyl vs dodecyl). Additionally, the other two substituents that are in positions 2 and 7 of the fluorene unit are far away from the chiral sp^3 center and thus contribute very little to the overall chirality of the monomers. Therefore, this minor substitution effect together with the rigidity of the fluorene structure and the steric hindrance of the chiral C9 center lead to the low response of the chiral monomers to circularly polarized light. To further interpret the observed CD spectra of the monomers, the time dependent (TD) DFT calculations were used to simulate the absorption and CD spectra and to determine the transitions in the spectra (see the Supporting Information). The observed CD peak in the experimental spectra of the monomers at ~310 nm (Figure 4a) corresponds to the minor peak in the calculated CD spectra, which can be attributed to the HOMO → LUMO+1 transition (Figure S33).

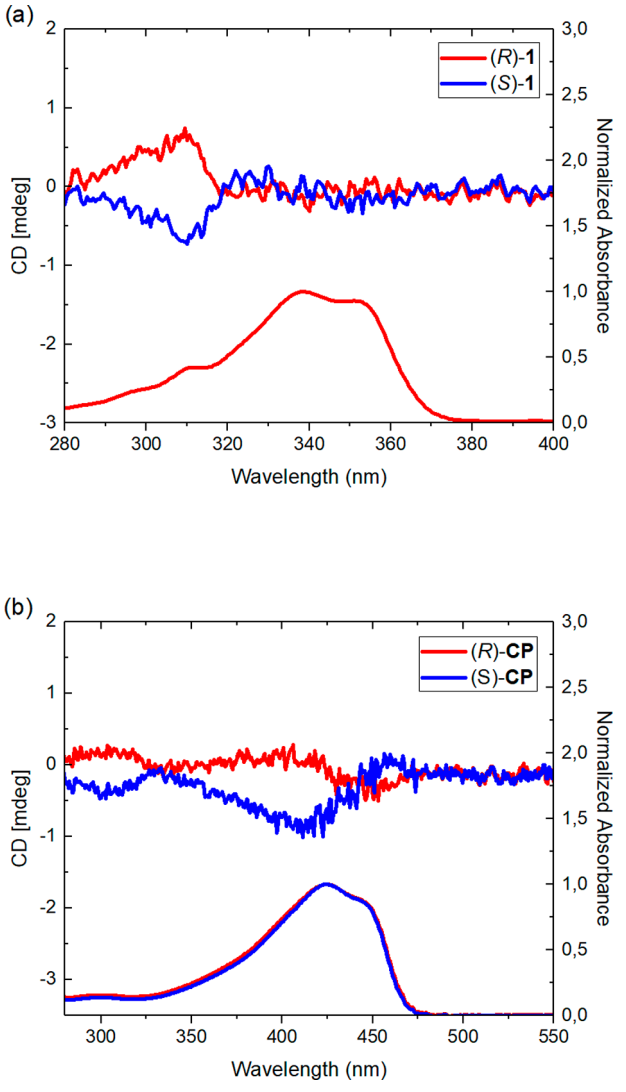

Figure 4. CD (top) and absorption (bottom) spectra of (a) monomers (*R*) 1 and (*S*) 1 and (b) polymers (*R*) CP and (*S*) CP. The samples were measured with a concentration of ~4 × 10^{-4} M in toluene at 25 °C.

Furthermore, the conformational flexibility and disorder of polymer chains in solution cause the very weak CD signal. As for the polymers, the chiroptical properties are normally created by a specific helical conformation. In our case, when (*R*) **CP** and (*S*) **CP** are dissolved and measured at 25 °C in toluene, which is a good solvent, the polymeric chains are flexible and adopt random coil like rather than ordered helical conformation. Fujiki and co workers[46] comprehensively studied the effects of chiral side chains of polyfluorene derivatives toward CD signs and magnitudes in solution, aggregates, and films. Inspired by that, we tried several cosolvents, but no enhancement of CD intensity was observed.

SWCNT Handedness Recognition by Chiral Polymers (*R*)-CP and (*S*)-CP. CoMoCAT SWCNTs (Signis SG65i, CHASM Advanced Materials Inc.) were used as raw material and processed with chiral homopolymers (*R*) **CP** and (*S*) **CP**. Each pair of enantiomeric samples and spectra discussed below are from one parallel trial. The absorption spectra of chiral polymer wrapped SWCNTs are shown in Figure 5, while the one of pristine SWCNTs dispersed in toluene is displayed in the Supporting Information.

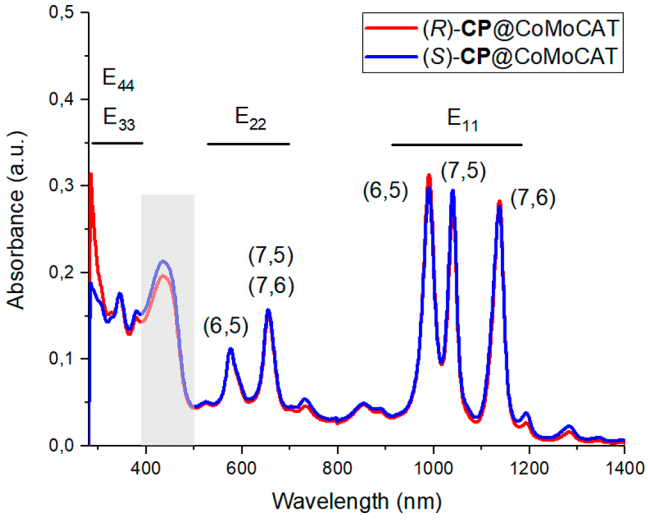

Figure 5. Absorption spectra of chiral polymer (*R*) CP and (*S*) CP dispersed CoMoCAT SWCNTs. The highlighted gray area corresponds to the absorption region of the neat polymer. All samples were measured in toluene at 25 °C.

After polymer wrapping and the subsequent removal of excess polymer, the absorption spectra of polymer wrapped SWCNTs exhibit sharp electronic absorption peaks and flat baselines when compared to those of pristine tubes (see Figure S36), which are associated with well dispersed samples of individually sus pended carbon nanotubes. The absorption peaks in semi conducting E_{11} and E_{22} regions in Figure 5 are labeled with chiral indices (*n*,*m*), indicating that both (*R*) **CP** and (*S*) **CP** disperse mainly (6,5), (7,5), and (7,6) s SWCNTs with comparable intensity. The polymer region between 400 and 500 nm might partially overlap with the E_{33} of (7,5) and (7,6) tubes but not with the E_{33} transition of the (6,5) tubes, which is assigned the sharp peak at 345 nm. For better interpretation of the overlapped area, we plotted the absorption spectra of polymer wrapped CNTs together with the neat polymer, as shown in Figure S37. The photoluminescence excitation (PLE) maps in Figure 6 confirm the similar performance of both chiral polymers to wrap mainly the three chiral tubes. The content of these (6,5), (7,5), and (7,6) SWCNTs is calculated according to the relative intensity of those three chiral indices in the PLE maps. For both samples, the relative content of (6,5), (7,5), and (7,6) SWCNTs is approximately 30%, 40%, and 30%, respectively.

On the basis of these results of PLE maps and absorption spectra, one can conclude that both chiral (*R*) **CP** and (*S*) **CP** polymers have identical wrapping ability and disperse preferentially semiconducting (6,5), (7,5), and (7,6) SWCNTs. AFM images prove that the SWCNTs in both samples are individualized with an average length of about 300 nm (see Figures S38 and S39). Moreover, the Raman spectra confirm the absence of metallic tubes in both samples (see Figures S40 and S41).

On the basis of the previous results, it is not necessary to remove the chiral polymers wrapped around the tubes and redisperse the sample with achiral polymer **ACP** before performing the CD and UV−vis experiments in order to obtain all four E_{ii} peaks of the SWCNT interband transitions, because the absorption peak of the polymer itself (highlighted in gray in Figure 5) is outside the characteristic E_{ii} tube transitions and the CD spectrum of the neat polymer is very weak (Figure 4b) and

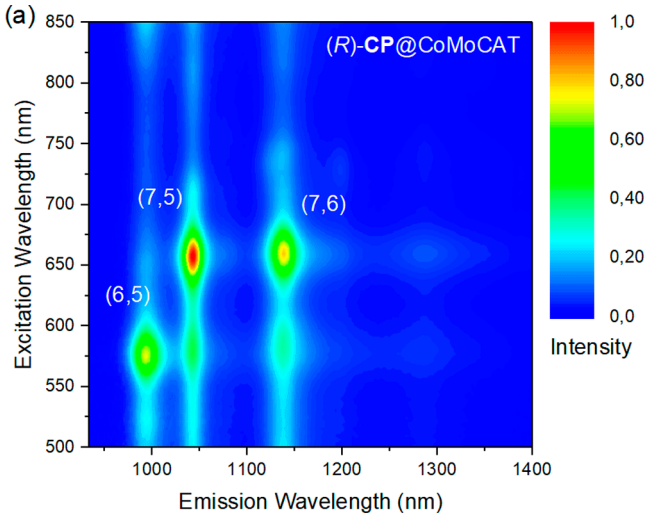

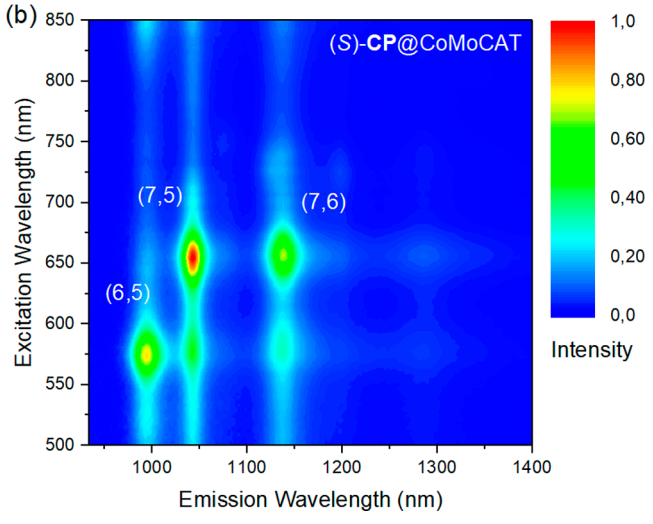

Figure 6. PLE maps of chiral polymer (a) (*R*) CP and (b) (*S*) CP dispersed CoMoCAT SWCNTs in toluene at room temperature. The intensities of the spots are normalized.

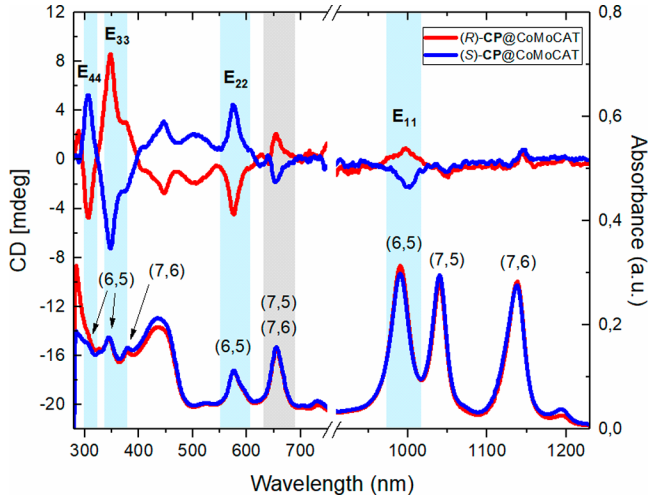

Figure 7. UV−vis NIR absorption and CD spectra of chiral polymer (*R*) CP and (*S*) CP dispersed CoMoCAT SWCNTs. All samples were measured in toluene at 25 °C.

does not affect the obtained results of handedness sorted nanotubes. Therefore, we measured the CD and absorption spectra before removing the chiral polymers, and the results are given in Figure 7.

The alternating positive and negative signs as well the mirror symmetry of the CD spectra indicate that we obtained two enantiomerically enriched samples. In the UV−vis region, the highlighted (Figure 7, blue) and labeled semiconducting transition bands E_{22}, E_{33}, and E_{44} fit well with the published results of the (6,5) SWCNT enantiomers.[47] On the basis of the reported data and the IUPAC terminology,[48,49] we assigned the (6,5) enantiomer, which gives a positive or negative E_{22} CD peak at 576 nm, as left handed (*M*) (blue plot) or right handed (*P*) (red plot) enantiomers, respectively. The small shoulders at 376 nm in the CD spectra belongs to the E_{33} transition of (7,6) SWCNT, and the broad peaks between 395 and 540 nm correspond to the cross polarized E_{ij} transition of (6,5) SWCNT.[31] (7,5) and (7,6) SWCNTs have E_{22} transition energies of 1.90 and 1.89 eV. respectively,[50] so that they share the peak at 654 nm in the absorption spectra, as highlighted in gray. However, the intensity of the E_{22} transition peak of the (7,5) and (7,6) tubes in the corresponding CD region (gray) is significantly lower than expected when compared to the E_{22} peak intensity of (6,5) SWCNTs at 576 nm. In addition, the CD peaks in this gray area are more likely attributed to the E_{21} transition of the (6,5) SWCNTs.[47] To explain this phenomenon, we need to first categorize all three tube species into Type 1 or Type 2 SWCNTs. According to Kataura and co workers,[31] (6,5) and (7,6) are Type 1 SWCNTs whereas (7,5) is a Type 2 SWCNT. More importantly, Type 1 and Type 2 SWCNTs with a specific handedness have opposite signs of the CD signals, and this statement is supported by theoretical calculations of the CD spectra.[51] In our case, the hypothesis is that each chiral polymer extracts all three nanotube species with similar handedness preferentially, so that the E_{22} CD signals of (7,5) and (7,6) SWCNTs might cancel each other, in particular because both samples with the same handedness are present in similar concentrations. Therefore, in the gray area, we can probably only observe the E_{21} transition of the (6,5) SWCNT. Moreover, the presence of the E_{33} peak from (7,6) enantiomers at 376 nm in the CD spectra proves that the handedness recognition of the chiral polymers is not limited to (6,5) SWCNT only. On the basis of the CD results in the UV−vis region and the theoretical calculations reported below, it is clear that the (*R*) **CP** polymer selectively extracts (*P*) (6,5), (*P*) (7,6), and (*P*) (7,5) SWCNTs, whereas the (*S*) **CP** polymer selectively extracts (*M*) (6,5), (*M*) (7,6), and (*M*) (7,5) SWCNTs. In the NIR region, the highlighted CD peaks belong to the E_{11} transition of the (6,5) enantiomers, and the signs are consistent with the alternating behavior of the E_{ii} CD signals of both (6,5) enantiomers. However, no symmetric signals were obtained from (7,5) and (7,6) enantiomers in the E_{11} transition region. A possible explanation for this phenomenon may be the low sensitivity of the detector and the high noise level of the CD spectra in the NIR region.

In order to determine the optical purity of the enantiomerically separated samples in terms of the (6,5) SWCNT enantiomers, we first applied the following eq 1:

$$CD_{norm} = (CD_{raw}/L_{CD})/(A_{E22}/L_{abs}) \quad (1)$$

where CD_{norm} and CD_{raw} are the CD values of the E_{22} transition peaks of the (6,5) SWCNT after and before normalization, A_{E22} is the absorbance at the E_{22} transition of the (6,5) SWCNT, L_{CD} and L_{abs} are the optical path lengths (cm) of the cell used for the CD and absorption analysis.[52] The calculated CD_{norm} in this work is −39 mdeg for (*P*) (6,5) SWCNT in the (*R*) **CP**@CoMoCAT sample and +40 mdeg for (*M*) (6,5) SWCNT in the (*S*) **CP**@CoMoCAT sample, indicating that the chiral polymers have the same handedness recognition ability owing to their all (*R*) and all (*S*) configurations. The obtained CD_{norm} values are higher than those reported by Weisman and co workers[29] using the DGU method (±36 mdeg) and Nakashima and co workers[38] using chiral copolymer wrapping (+24 mdeg) but lower than those reported by Kataura and co workers[31] using gel column chromatography (+93, −85 mdeg) and Zheng and co workers[32] using DNA differentiation (±84 mdeg).

Furthermore, we applied eqs 2 and 3 to estimate the enantiomeric purity (EP) of the samples with calculated CD_{norm} values, as reported by Kataura and co workers using gel column chromatography for handedness sorting of the CNTs and the subsequent redispersion of the CNT enantiomers in a Flavin mononucleotide aqueous solution,[47]

$$EP(M)\text{-}(6,5)(\%) = 50 + \alpha CD_{norm} \quad (2)$$

$$EP(P)\text{-}(6,5)(\%) = 50 - \alpha CD_{norm} \quad (3)$$

Here, α is a linear scaling factor that is set as 0.421 ± 0.030 $mdeg^{-1}$. Thus, the EP values of the (*R*) **CP**@CoMoCAT and (*S*) **CP**@CoMoCAT samples become (66.4 ± 1.2)% and (66.8 ± 1.2)%, respectively.

Note that these two enantiomeric samples were prepared in one parallel trial. In order to obtain comparable results from (*R*) **CP** and (*S*) **CP** polymers, it is necessary to maintain strictly the same conditions during the preparation and sorting process. However, even a slight change in the parallel separation could cause a different performance of the chiral polymers, which affects the wrapping yield and the enantiomeric purity of the obtained samples. For instance, the sonication strength in a glass vial may be subject to fluctuations when the vial is placed in different positions or depths inside the sonication bath. Moreover, a curved baseline in the CD spectrum could cause large discrepancies in the calculation of the EP. Due to these facts, it is difficult to obtain absolutely the same enantiomeric purities for the pair of enantiomers in one parallel trial and to absolutely maintain their reproducibility. For better interpretation of the CD spectra and comparison with other published results, we selected and show in the main text only the pair of enantiomers giving similar EP and fully symmetric CD spectra (Figure 7). CD spectra of other batches are in Figure S44. It is worth noting that for all batches the lowest EP value obtained for the CNT enantiomers is 57% and the highest one is 89% (see the Supporting Information and Figure S44). To the best of our knowledge, these enantiomeric purities ranging from 57% to 89% are so far the highest values achieved for enantiomeric separation of SWCNTs using a chiral polymer. In the Supporting Information, we additionally show absorption and CD spectra (Figure S44) of one pair of samples from two different and not absolutely equal batches. The calculated CD_{norm} value in Figure S44a is −93 mdeg for the (*P*) (6,5) SWCNT in the (*R*) **CP**@CoMoCAT sample and +59 mdeg for the (*M*) (6,5) SWCNT in the (*S*) **CP**@CoMoCAT sample after the baseline correction (zero value line), corresponding to the EP(%) values of (89.2 ± 2.8)% and (74.8 ± 1.2)%, respectively. Similar discrepancies in the calculated EP values for the pair of SWCNT enantiomers have been observed in the previous studies.[28,29,31,32,38,52] On the basis of those findings, we believe that our chiral polymers (*R*) **CP** and (*S*) **CP** are able to selectively extract left handed and right handed SWCNTs from raw CNT material with comparable enantiomeric purity to that recently published by Kataura and co workers[31] and Zheng and co workers[32] but using a low cost methodology based on removable chiral polymer sorting.

Cleavage of the Polymer. After the separation process, the wrapping polymers can be quantitatively removed by cleaving the imine bonds (C═N) in the polymer backbone with a catalytic amount of acid, yielding dispersant free single handed s SWCNTs. Upon an addition of a catalytic amount of acid, the polymer quickly degrades into oligomers and monomers and thus detaches from the nanotubes and causes the quantitative precipitation of naked SWCNTs. The advantage of this dynamic imine bond cleavage approach is that the monomers can be recovered almost quantitatively and be engaged in the synthesis of the next chiral polymers.[42]

In the absorption spectra, as shown in Figure S34, the polymer peak disappears after acid treatment and washing of monomers with toluene. The absence of the absorption band in the released SWCNT sample between 400 and 500 nm also indicates the absence of metallic SWCNTs. Further kinetic and concentration studies of polyimine cleavage to the corresponding monomers are detailed in Figure S35. The quantitative cleavage of the polymer was further corroborated by X ray photoelectron spectroscopy (XPS) measurements, where the N 1s peak attributed to the N atoms in the polyimine disappeared in the released SWNT sample (see Figure S42).

Rewrapping of Naked SWCNTs with Nonchiral Polymer. In order to confirm that our chiral polymers (*R*) **CP** and (*S*) **CP** have only minor effects on the CD spectra and the obtained CD signal is intrinsic to the SWCNT enantiomers, we degraded the chiral polymer and subsequently rewrapped the enantiomerically pure CNTs with the commercially available achiral PFO Bpy polymer, which has been reported to have a specific selectivity for the (6,5) nanotubes.[24] As shown in Figure 8, negligible changes in CD intensities of E_{22}, E_{33}, and E_{44} transitions are observed, confirming that the CD signal is intrinsic to the nanotube sample and not induced by the chiral polymers helically wrapped around a SWCNT. The procedure for the rewrapping and redispersion of triggered SWCNTs with achiral polymer PFO Bpy is given in the Supporting Information.

Molecular Dynamics Simulation. In order to understand the origin of the wrapping selectivity toward handedness sorting of SWCNTs observed in the experiments, we performed molecular mechanics simulations. Because the full conformational relaxation of the polymer around the SWCNT is a very slow process, we first computed low energy conformations of the twisted polymer using Monte Carlo (MC) simulations. Statistical fluctuations in the MC simulations automatically generate conformations with two wrapping directions, *i.e.*, clockwise (+) and anticlockwise (−). For each polymer−CNT complex, two wrapping directions have been considered as the initial conformations for MD simulation. We then relaxed these conformations in MD simulations modeling (*R*) **CP** *M* (6,5) and (*S*) **CP** *M* (6,5) complexes. Structures extracted from the last 1 ns of the MD simulations for four different systems are shown in Figure 9.

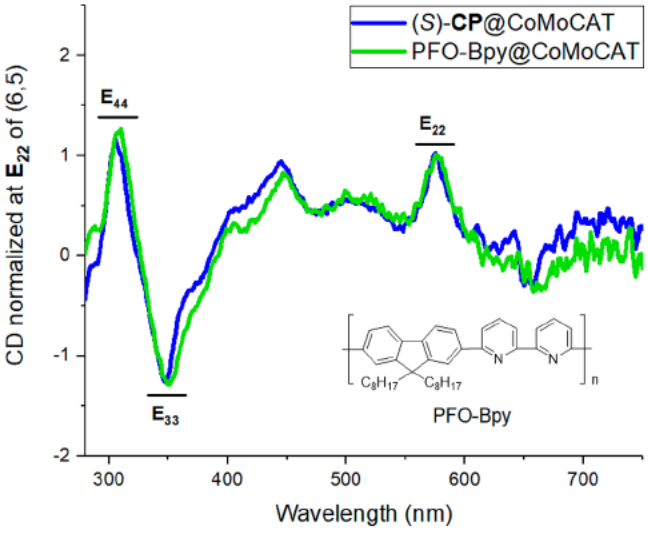

Figure 8. CD spectra of chiral polymer (*S*) CP dispersed SWCNTs and achiral PFO Bpy polymer redispersed SWCNTs after trigger ing. The structure of the PFO Bpy polymer is shown in the figure. All samples were measured in toluene at 25 °C.

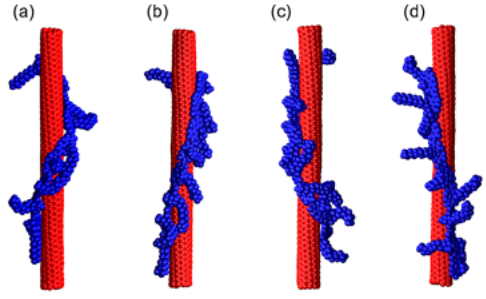

Figure 9. Structures extracted from MD simulation (solvent molecules are hidden) for (a) (*R*) CP *M* (6,5) clockwise wrapped, (b) (*S*) CP *M* (6,5) clockwise wrapped, (c) (*R*) CP *M* (6,5) anticlockwise wrapped, and (d) (*S*) CP *M* (6,5) anticlockwise wrapped.

The binding energy (E_{bind}) of the wrapped SWCNT was calculated by eq 4:

$$E_{bind} = E_{poly\text{-}CNT\text{-}sol} - E_{poly\text{-}sol} - E_{CNT\text{-}sol} - E_{poly} - E_{CNT} - E_{sol} \quad (4)$$

where $E_{poly\text{-}CNT\text{-}sol}$ is the total energy, $E_{poly\ sol}$ is the interaction energy between polymer and solvent, and $E_{CNT\text{-}sol}$ is the interaction energy between SWCNT and solvent. E_{poly}, E_{CNT}, and E_{sol} are the energies of free polymer, SWCNT, and solvent, respectively. The calculated potential energies are summarized in Table 1.

We found more favorable binding energies for the (*R*) CP *P* (6,5) and (*S*) CP *M* (6,5) complexes compared to the (*S*) CP *P* (6,5) and (*R*) CP *M* (6,5) complexes in both cases where the polymer wraps the SWCNT in the clockwise (+) or anticlockwise (−) directions. These results are in full agreement with the previous experimental CD results, where (*R*) CP polymer preferentially extracts right handed (*P*) SWCNTs and (*S*) CP polymer preferentially extracts left handed (*M*) SWCNTs.

Since it is expected that the binding energy for such systems is influenced by specific noncovalent interaction of the polymer and SWCNT,[53] the contributions of the $\pi-\pi$ stacking interaction to the binding energies are also reported for each complex in Table 1. The calculated $E_{\pi-\pi}$ indicates that the increased tendency for (*R*) CP (or (*S*) CP) to wrap around the *P* (6,5) (or *M* (6,5)) SWCNT originates from an increased $\pi-\pi$ interaction between polymer and SWCNT, which is made possible by the favorable geometry of the polymer aromatic rings to interact with the SWCNT surface. Furthermore, free energy calculations show that (*S*) CP interacts more favorably with the *M* (6,5) SWCNT in the anticlockwise direction (−) than in the clockwise (+) direction (Table 1 and Figure 9d). In this case, the backbone of (*S*) CP lies along the vector line of the *M* (6,5) SWCNT, thus maximizing the contacts as well as the $\pi-\pi$ interactions between the polymer and SWCNT aromatic rings, while the long side chains stretch into the solvent, thus reducing the steric effects, as shown in Figure 9b. Hence, it can be concluded that maximizing the $\pi-\pi$ stacking nonbonded interactions along with minimizing the steric effects of the long side chains are the driving forces for the selective interaction between chiral polymers and SWCNT enantiomers.

Table 1. Binding Energies (E_{bind}) and Contributions of $\pi-\pi$ Stacking Interactions ($E_{\pi-\pi}$) for Each Enantiomeric Complex with Polymer Wrapping Direction Clockwise (+) or Anticlockwise (−)[a]

complex	E_{bind} (+)	$E_{\pi-\pi}$ (+)	E_{bind} (−)	$E_{\pi-\pi}$ (−)
(*R*)-CP-*M*-(6,5)	51	125	105	68
(*R*)-CP-*P*-(6,5)	386	494	165	311
(*S*)-CP-*M*-(6,5)	165	311	386	494
(*S*)-CP-*P*-(6,5)	105	68	51	125

[a]All energies are averaged from the last 2 ns of MD simulations and are reported in kcal/mol.

Owing to the all (*R*) or all (*S*) configuration of the chiral polymers, the obtained binding energy difference between (*R*) CP *P* (6,5) and (*R*) CP *M* (6,5) complexes in the clockwise direction or between (*S*) CP *M* (6,5) and (*S*) CP *P* (6,5) complexes in the anticlockwise direction is 437 kcal/mol. This value is significantly higher than the one calculated previously for binaphthol−fluorene based chiral copolymers, supporting the tight geometry of the chiral polymer along the carbon nanotubes and thus increasing the difference between these two wrapping scenarios.[38] The assignment of positive and negative E_{22} CD peaks of the (6,5) SWCNTs to the left handed (*M*) and right handed (*P*) enantiomers is therefore also strongly supported by these calculations.

CONCLUSIONS

We designed and synthesized all (*R*) and all (*S*) acid cleavable chiral polyfluorenes with the quaternary stereocenter on each monomeric unit for handedness sorting of semiconducting SWCNTs. Each chiral polymer selectively extracts either left handed or right handed (6,5), (7,5), and (7,6) s SWCNTs in one pot from commercially available CoMoCAT SWCNTs with a high enantiomeric excess according to its respective preference. In the experimental CD spectra, we clearly observed all four typical E_{11}, E_{22}, E_{33}, and E_{44} transitions of the polymer wrapped optically enriched (6,5) SWCNT enantiomers, while the E_{22} CD signals of the (7,5) and (7,6) SWCNTs have opposite signs and cancel each other due to the different type of SWCNT index. Quantitative removal of the chiral polymer was achieved by an acid treatment, and the released nanotubes can be easily rewrapped with a nonchiral polymer. Results obtained from all atom MD simulations are in good qualitative agreement

with the experimental observations, indicating that the (*R*) CP polymer tends to wrap around the right handed (*P*) (6,5) SWCNT in the clockwise direction while the (*S*) CP polymer tends to wrap around the left handed (*M*) (6,5) SWCNT in the anticlockwise direction. Our approach to sort enantiomerically pure polymer free s SWCNTs is beneficial in terms of low cost, high selectivity, and high purity of sorted nanotubes. It provides easier access to handedness selected SWCNTs with better electronic properties for future electronic applications.

EXPERIMENTAL SECTION

Synthesis of Polymers. The detailed synthetic steps for the racemic monomer **1** are given in the Supporting Information. All three polyimines (**ACP**, (*R*) **CP**, and (*S*) **CP**) were synthesized by the polycondensation reaction with the same procedure starting from **1**, (*R*) **1**, and (*S*) **1**, respectively. The synthetic procedure for the achiral **ACP** polymer is described as an example, while the synthetic details for the chiral polymers are given in the Supporting Information. For **ACP**, a 25 mL Schlenk flask was charged with **1** (100 mg, 0.20 mmol) and anhydrous DCM (8 mL) under an argon atmosphere. Trifluoroacetic acid (1.6 mL, 99%) and thioanisole (48 μL, 0.40 mmol, 2.0 equiv) were subsequently added, and the mixture was stirred at room temperature overnight. The resulting red mixture was quenched with saturated $NaHCO_3$ solution and extracted with DCM. The combined organic phase was washed with brine, dried over $MgSO_4$, and filtrated. All solvents were removed under reduced pressure, and the residue was polymerized directly in the flask at 100 °C under vacuum ($\sim 10^{-2}$ mbar) for 48 h. 77 mg of a yellow polymeric film was obtained as the final product in 98%. ^{1}H NMR ($CDCl_3$, 500 MHz): δ ppm = 8.66 (s, 1H), 8.01−7.80 (m, 4H), 7.32 (m, 2H), 2.13 (m, 4H), 1.25−1.09 (m, 18H), 0.85 (t, 3H), 0.73 (m, 2H), 0.37 (m, 3H); GPC (in THF): M_n = 90 kDa, M_w = 287 kDa, PDI = 3.14.

Enantiomeric Separation of s-SWCNTs. The pristine material CoMoCAT SWCNTs were purchased from CHASM Advanced Materials (LOT# SG65i L64). The typical procedure for wrapping with our polyimine polymers is as follows: 0.5 mg of CoMoCAT SWCNTs and 1.5 mg of polymer were dispersed in 5 mL of toluene under ice water bath sonication for 6 h. The temperature during the sonication was kept around 15 °C. The suspension was then centrifuged at 17 920 RCF for 1 h, and the upper solution was collected and further centrifuged at 112 000 RCF for 3 h. The precipitate was redispersed, sonicated, and centrifuged again to remove the polymer excess in toluene. The resulting samples were dispersed in 1 mL of toluene for characterization. The procedure for acid triggered polymer cleavage of the wrapped samples is given in the Supporting Information. The PFO Bpy polymer used for rewrapping of the released SWCNTs was purchased from American Dye Source, Inc. (ADS153UV, Lot# 15L007A1).

Computational Method. We utilized a fully atomistic molecular model in our simulations, which treats all atoms and solvent explicitly. (6,5) SWCNTs of 11 nm length were generated as model SWCNTs using VMD,[54] and the unsaturated boundary effect was avoided by adding hydrogen atoms at the ends of the tubes. A trimer structure of the polymer optimized using the B3 LYP exchange correlation functional[55,56] and the def2 SV(P) basis set[57,58] using TURBO MOLE[59] were used to generate a polymer of 10 repeating units using AmberTools.[60] Monte Carlo sampling was performed to obtain the lowest energy configuration of the polymer using SIMONA,[61] where the torsions of the molecule were sampled *via* the backbone dihedral angles to create a helical conformation that fits around the SWCNT. To create (*R*) and (*S*) polymers, the backbone configuration from Monte Carlo calculations was kept completely the same but the side chains were substituted with different chiralities.

The solvent molecules (toluene) were added to the box of size 5 × 5 × 15 nm (~29 000 atoms) modeled with the experimental density of 0.87 g/mL using PACKMOL.[62] MD simulations were carried out with LAMMPS using the COMPASS force field.[63−65] After minimizing and eliminating any voids in the system, a 1 ns NPT simulation was carried out to equilibrate the system at 1 atm and 300 K. These equilibration steps were followed by a 4 ns production run to collect statistical data. In the production run, the time step was 1.0 fs; structures were saved every 0.2 ps, and cubic periodic boundary conditions (PBCs) were applied in all directions. Electrostatic interactions were calculated using the particle−particle particle mesh method (pppm) with a real space cutoff of 12 Å.[66]

Instrumentation. The enantiomers of **1** were separated by chiral flash chromatography using a SHIMADZU LC 20AT HPLC, which was equipped with a CHIRALPAK IB N 5 HPLC column (*n* heptane/isopropanol = 96:4) and a UV−vis detector. The molecular weights of the polymers were measured by an Agilent HPLC system equipped with two PLgel GPC/SEC columns (5 μm, 300 × 7.5 mm), and the polystyrene molecular weight standards have been used. The sonication process was carried out in a water bath sonicator, which was purchased from VWR (Model USC500T) with an output frequency of 45 kHz. The absorption spectra were recorded on a Varian Cary 500 UV−vis NIR spectrophotometer in a quartz cuvette with a path length of 1 cm. The CD spectra were recorded on a JASCO J 1500 CD spectrometer with a PMT detector and a Xe lamp as the light source for the UV−vis region. For the NIR region, an InGaAs detector and a halogen lamp as the light source were used. All CD spectra were acquired with a 2 s digital integration time and 4 nm bandwidth in a quartz cuvette with a path length of 1 cm. The PLE maps were measured in the emission range of 934−1700 nm and excitation range of 500−950 nm (in 3 nm steps) using a modified FTIR spectrometer (Bruker IFS66) equipped with a liquid nitrogen cooled Ge photodiode and a monochromatized excitation light source.

ASSOCIATED CONTENT

Supporting Information

The Supporting Information is available free of charge at https://pubs.acs.org/doi/10.1021/acsnano.0c09235.

> Monomer and polymer synthesis in detail, characterizations of all molecules, procedure for acid based triggering of the wrapped SWCNTs, procedure for the redispersion of triggered SWCNTs with achiral polymer, details of the Mosher's method to determine the absolute configuration of enantiomeric monomers using NMR analysis, additional absorption, Raman, AFM, and XPS results, theoretical calculations of absorption, and CD spectra of enantiomers (PDF)

AUTHOR INFORMATION

Corresponding Authors

Michal Valášek − *Institute of Nanotechnology, Karlsruhe Institute of Technology, 76021 Karlsruhe, Germany;* orcid.org/0000 0001 9382 6327; Email: michal.valasek@kit.edu

Manfred M. Kappes − *Institute of Nanotechnology, Karlsruhe Institute of Technology, 76021 Karlsruhe, Germany; Institute of Quantum Materials and Technologies and Institute of Physical Chemistry, Karlsruhe Institute of Technology, 76021 Karlsruhe, Germany;* orcid.org/0000 0002 1199 1730; Email: manfred.kappes@kit.edu

Marcel Mayor − *Institute of Nanotechnology, Karlsruhe Institute of Technology, 76021 Karlsruhe, Germany; Department of Chemistry, University of Basel, 4056 Basel, Switzerland; Lehn Institute of Functional Materials, School of Chemistry, Sun Yat Sen University, Guangzhou, Guangdong 510275, China;* orcid.org/0000 0002 8094 7813; Email: marcel.mayor@unibas.ch

Authors

Liang Xu – *Institute of Nanotechnology, Karlsruhe Institute of Technology, 76021 Karlsruhe, Germany*

Frank Hennrich – *Institute of Nanotechnology, Karlsruhe Institute of Technology, 76021 Karlsruhe, Germany; Institute of Quantum Materials and Technologies, Karlsruhe Institute of Technology, 76021 Karlsruhe, Germany*

Elaheh Sedghamiz – *Institute of Nanotechnology, Karlsruhe Institute of Technology, 76021 Karlsruhe, Germany;* orcid.org/0000 0003 3998 9701

Montserrat Penaloza Amion – *Institute of Nanotechnology, Karlsruhe Institute of Technology, 76021 Karlsruhe, Germany*

Daniel Häussinger – *Department of Chemistry, University of Basel, 4056 Basel, Switzerland;* orcid.org/0000 0002 4798 0072

Wolfgang Wenzel – *Institute of Nanotechnology, Karlsruhe Institute of Technology, 76021 Karlsruhe, Germany*

Author Contributions

The manuscript was written through contributions of all authors. All authors have given approval to the final version of the manuscript.

Notes

The authors declare no competing financial interest.

ACKNOWLEDGMENTS

The authors are very grateful to Dr. Leonardo Velasco Estrada who performed the XPS measurements. The authors acknowl edge the support by the Helmholtz Research Program STM (Science and Technology of Nanosystems). The authors also thank the Institute of Nanotechnology (INT), Karlsruhe Institute of Technology (KIT) for ongoing support. E.S. and W.W. acknowledge support by the Deutsche Forschungsge meinschaft (DFG, German Research Foundation) under Germany's Excellence Strategy *via* the Excellence Cluster 3D Matter Made to Order (EXC 2082/1 390761711) and by the Carl Zeiss Foundation through the "Carl Zeiss Focus@ HEiKA". M.P. A. was supported by a grant from the Deutscher Akademischer Austauschdienst (DAAD; 91683960). M.M. and M.M.K. acknowledge support by a joint SNF (200021L 150188) DFG (KA 972/9 1) project. M.M. acknowledges support by the 111 project (90002 18011002).

REFERENCES

(1) Iijima, S.; Ichihashi, T. Single Shell Carbon Nanotubes of 1 Nm Diameter. *Nature* **1993**, *363* (6430), 603–605.

(2) Saito, R.; Dresselhaus, G.; Dresselhaus, M. S. *Physical Properties of Carbon Nanotubes*; Imperial College Press: London, 1998.

(3) Treacy, M. M. J.; Ebbesen, T. W.; Gibson, J. M. Exceptionally High Young's Modulus Observed for Individual Carbon Nanotubes. *Nature* **1996**, *381* (6584), 678–680.

(4) Ouyang, M.; Huang, J. L.; Lieber, C. M. Fundamental Electronic Properties and Applications of Single Walled Carbon Nanotubes. *Acc. Chem. Res.* **2002**, *35* (12), 1018–1025.

(5) Weisman, R. B.; Bachilo, S. M. Dependence of Optical Transition Energies on Structure for Single Walled Carbon Nanotubes in Aqueous Suspension: An Empirical Kataura Plot. *Nano Lett.* **2003**, *3* (9), 1235–1238.

(6) O'Connell, M. J.; Bachilo, S. M.; Huffman, C. B.; Moore, V. C.; Strano, M. S.; Haroz, E. H.; Rialon, K. L.; Boul, P. J.; Noon, W. H.; Kittrell, C.; Ma, J.; Hauge, R. H.; Weisman, R. B.; Smalley, R. E. Band Gap Fluorescence from Individual Single Walled Carbon Nanotubes. *Science* **2002**, *297* (5581), 593–596.

(7) Hennrich, F.; Li, W.; Fischer, R.; Lebedkin, S.; Krupke, R.; Kappes, M. M. Length Sorted, Large Diameter, Polyfluorene Wrapped Semi conducting Single Walled Carbon Nanotubes for High Density, Short Channel Transistors. *ACS Nano* **2016**, *10* (2), 1888–1895.

(8) Nougaret, L.; Happy, H.; Dambrine, G.; Derycke, V.; Bourgoin, J. P.; Green, A. A.; Hersam, M. C. 80 GHz Field Effect Transistors Produced Using High Purity Semiconducting Single Walled Carbon Nanotubes. *Appl. Phys. Lett.* **2009**, *94* (24), 243505.

(9) Joo, Y.; Brady, G. J.; Kanimozhi, C.; Ko, J.; Shea, M. J.; Strand, M. T.; Arnold, M. S.; Gopalan, P. Polymer Free Electronic Grade Aligned Semiconducting Carbon Nanotube Array. *ACS Appl. Mater. Interfaces* **2017**, *9* (34), 28859–28867.

(10) Hennrich, F.; Lebedkin, S.; Malik, S.; Tracy, J.; Barczewski, M.; Rösner, H.; Kappes, M. Preparation, Characterization and Applications of Free Standing Single Walled Carbon Nanotube Thin Films. *Phys. Chem. Chem. Phys.* **2002**, *4* (11), 2273–2277.

(11) Kang, S. J.; Kocabas, C.; Ozel, T.; Shim, M.; Pimparkar, N.; Alam, M. A.; Rotkin, S. V.; Rogers, J. A. High Performance Electronics Using Dense, Perfectly Aligned Arrays of Single Walled Carbon Nanotubes. *Nat. Nanotechnol.* **2007**, *2* (4), 230–236.

(12) Hu, L.; Hecht, D. S.; Grüner, G. Carbon Nanotube Thin Films: Fabrication, Properties, and Applications. *Chem. Rev.* **2010**, *110* (10), 5790–5844.

(13) Star, A.; Lu, Y.; Bradley, K.; Grüner, G. Nanotube Optoelectronic Memory Devices. *Nano Lett.* **2004**, *4* (9), 1587–1591.

(14) Avouris, P.; Freitag, M.; Perebeinos, V. Carbon Nanotube Photonics and Optoelectronics. *Nat. Photonics* **2008**, *2* (6), 341–350.

(15) Gaviria Rojas, W. A.; Hersam, M. C. Chirality Enriched Carbon Nanotubes for Next Generation Computing. *Adv. Mater.* **2020**, *32* (41), 1905654.

(16) Hitosugi, S.; Yamasaki, T.; Isobe, H. Bottom Up Synthesis and Thread in Bead Structures of Finite (n,0) Zigzag Single Wall Carbon Nanotubes. *J. Am. Chem. Soc.* **2012**, *134* (30), 12442–12445.

(17) Omachi, H.; Matsuura, S.; Segawa, Y.; Itami, K. A Modular and Size Selective Synthesis of [n]Cycloparaphenylenes: A Step toward the Selective Synthesis of [n,n] Single Walled Carbon Nanotubes. *Angew. Chem., Int. Ed.* **2010**, *49* (52), 10202–10205.

(18) Sanchez Valencia, J. R.; Dienel, T.; Gröning, O.; Shorubalko, I.; Mueller, A.; Jansen, M.; Amsharov, K.; Ruffieux, P.; Fasel, R. Controlled Synthesis of Single Chirality Carbon Nanotubes. *Nature* **2014**, *512* (7512), 61–64.

(19) Arnold, M. S.; Stupp, S. I.; Hersam, M. C. Enrichment of Single Walled Carbon Nanotubes by Diameter in Density Gradients. *Nano Lett.* **2005**, *5* (4), 713–718.

(20) Arnold, M. S.; Green, A. A.; Hulvat, J. F.; Stupp, S. I.; Hersam, M. C. Sorting Carbon Nanotubes by Electronic Structure Using Density Differentiation. *Nat. Nanotechnol.* **2006**, *1* (1), 60–65.

(21) Liu, H.; Nishide, D.; Tanaka, T.; Kataura, H. Large Scale Single Chirality Separation of Single Wall Carbon Nanotubes by Simple Gel Chromatography. *Nat. Commun.* **2011**, *2*, 309.

(22) Wei, X.; Tanaka, T.; Hirakawa, T.; Wang, G.; Kataura, H. High Efficiency Separation of (6,5) Carbon Nanotubes by Stepwise Elution Gel Chromatography. *Phys. Status Solidi B* **2017**, *254* (11), 1700279.

(23) Zheng, M.; Jagota, A.; Strano, M. S.; Santos, A. P.; Barone, P.; Chou, S. G.; Diner, B. A.; Dresselhaus, M. S.; Mclean, R. S.; Onoa, G. B.; Samsonidze, G. G.; Semke, E. D.; Usrey, M.; Walls, D. J. Structure Based Carbon Nanotube Sorting by Sequence Dependent DNA Assembly. *Science* **2003**, *302* (5650), 1545–1548.

(24) Ozawa, H.; Ide, N.; Fujigaya, T.; Niidome, Y.; Nakashima, N. One Pot Separation of Highly Enriched (6,5) Single Walled Carbon Nanotubes Using a Fluorene Based Copolymer. *Chem. Lett.* **2011**, *40* (3), 239–241.

(25) Yang, F.; Wang, M.; Zhang, D.; Yang, J.; Zheng, M.; Li, Y. Chirality Pure Carbon Nanotubes: Growth, Sorting, and Character ization. *Chem. Rev.* **2020**, *120* (5), 2693–2758.

(26) Pu, C.; Xu, Y.; Liu, Q.; Zhu, A.; Shi, G. Enantiomers of Single Chirality Nanotube as Chiral Recognition Interface for Enhanced

Electrochemical Chiral Analysis. *Anal. Chem.* **2019**, *91* (4), 3015−3020.
(27) Peng, X.; Komatsu, N.; Bhattacharya, S.; Shimawaki, T.; Aonuma, S.; Kimura, T.; Osuka, A. Optically Active Single Walled Carbon Nanotubes. *Nat. Nanotechnol.* **2007**, *2* (6), 361−365.
(28) Green, A. A.; Duch, M. C.; Hersam, M. C. Isolation of Single Walled Carbon Nanotube Enantiomers by Density Differentiation. *Nano Res.* **2009**, *2* (1), 69−77.
(29) Ghosh, S.; Bachilo, S. M.; Weisman, R. B. Advanced Sorting of Single Walled Carbon Nanotubes by Nonlinear Density Gradient Ultracentrifugation. *Nat. Nanotechnol.* **2010**, *5* (6), 443−450.
(30) Liu, H.; Tanaka, T.; Kataura, H. Optical Isomer Separation of Single Chirality Carbon Nanotubes Using Gel Column Chromatog raphy. *Nano Lett.* **2014**, *14* (11), 6237−6243.
(31) Wei, X.; Tanaka, T.; Yomogida, Y.; Sato, N.; Saito, R.; Kataura, H. Experimental Determination of Excitonic Band Structures of Single Walled Carbon Nanotubes Using Circular Dichroism Spectra. *Nat. Commun.* **2016**, *7*, 12899.
(32) Ao, G.; Streit, J. K.; Fagan, J. A.; Zheng, M. Differentiating Left and Right Handed Carbon Nanotubes by DNA. *J. Am. Chem. Soc.* **2016**, *138* (51), 16677−16685.
(33) Nish, A.; Hwang, J. Y.; Doig, J.; Nicholas, R. J. Highly Selective Dispersion of Single Walled Carbon Nanotubes Using Aromatic Polymers. *Nat. Nanotechnol.* **2007**, *2* (10), 640−646.
(34) Berton, N.; Lemasson, F.; Tittmann, J.; Stürzl, N.; Hennrich, F.; Kappes, M. M.; Mayor, M. Copolymer Controlled Diameter Selective Dispersion of Semiconducting Single Walled Carbon Nanotubes. *Chem. Mater.* **2011**, *23* (8), 2237−2249.
(35) Gomulya, W.; Costanzo, G. D.; de Carvalho, E. J. F.; Bisri, S. Z.; Derenskyi, V.; Fritsch, M.; Fröhlich, N.; Allard, S.; Gordiichuk, P.; Herrmann, A.; Marrink, S. J.; dos Santos, M. C.; Scherf, U.; Loi, M. A. Semiconducting Single Walled Carbon Nanotubes on Demand by Polymer Wrapping. *Adv. Mater.* **2013**, *25* (21), 2948−2956.
(36) Lemasson, F.; Berton, N.; Tittmann, J.; Hennrich, F.; Kappes, M. M.; Mayor, M. Polymer Library Comprising Fluorene and Carbazole Homo and Copolymers for Selective Single Walled Carbon Nano tubes Extraction. *Macromolecules* **2012**, *45* (2), 713−722.
(37) Ozawa, H.; Fujigaya, T.; Niidome, Y.; Hotta, N.; Fujiki, M.; Nakashima, N. Rational Concept To Recognize/Extract Single Walled Carbon Nanotubes with a Specific Chirality. *J. Am. Chem. Soc.* **2011**, *133* (8), 2651−2657.
(38) Akazaki, K.; Toshimitsu, F.; Ozawa, H.; Fujigaya, T.; Nakashima, N. Recognition and One Pot Extraction of Right and Left Handed Semiconducting Single Walled Carbon Nanotube Enantiomers Using Fluorene Binaphthol Chiral Copolymers. *J. Am. Chem. Soc.* **2012**, *134* (30), 12700−12707.
(39) Wang, W. Z.; Li, W. F.; Pan, X. Y.; Li, C. M.; Li, L. J.; Mu, Y. G.; Rogers, J. A.; Chan Park, M. B. Degradable Conjugated Polymers: Synthesis and Applications in Enrichment of Semiconducting Single Walled Carbon Nanotubes. *Adv. Funct. Mater.* **2011**, *21* (9), 1643−1651.
(40) Norton Baker, B.; Ihly, R.; Gould, I. E.; Avery, A. D.; Owczarczyk, Z. R.; Ferguson, A. J.; Blackburn, J. L. Polymer Free Carbon Nanotube Thermoelectrics with Improved Charge Carrier Transport and Power Factor. *ACS Energy Lett.* **2016**, *1* (6), 1212−1220.
(41) Chortos, A.; Pochorovski, I.; Lin, P.; Pitner, G.; Yan, X.; Gao, T. Z.; To, J. W. F.; Lei, T.; Will, J. W.; Wong, H. S. P.; Bao, Z. Universal Selective Dispersion of Semiconducting Carbon Nanotubes from Commercial Sources Using a Supramolecular Polymer. *ACS Nano* **2017**, *11* (6), 5660−5669.
(42) Lei, T.; Chen, X.; Pitner, G.; Wong, H. S. P.; Bao, Z. Removable and Recyclable Conjugated Polymers for Highly Selective and High Yield Dispersion and Release of Low Cost Carbon Nanotubes. *J. Am. Chem. Soc.* **2016**, *138* (3), 802−805.
(43) Kanimozhi, C.; Brady, G. J.; Shea, M. J.; Huang, P.; Joo, Y.; Arnold, M. S.; Gopalan, P. Structurally Analogous Degradable Version of Fluorene−Bipyridine Copolymer with Exceptional Selectivity for Large Diameter Semiconducting Carbon Nanotubes. *ACS Appl. Mater. Interfaces* **2017**, *9* (46), 40734−40742.
(44) Dale, J. A.; Dull, D. L.; Mosher, H. S. α Methoxy .Alpha. Trifluoromethylphenylacetic Acid, a Versatile Reagent for the Determination of Enantiomeric Composition of Alcohols and Amines. *J. Org. Chem.* **1969**, *34* (9), 2543−2549.
(45) Dale, J. A.; Mosher, H. S. Nuclear Magnetic Resonance Enantiomer Regents. Configurational Correlations *via* Nuclear Magnetic Resonance Chemical Shifts of Diastereomeric Mandelate, *O* Methylmandelate, and α Methoxy α Trifluoromethylphenylacetate (MTPA) Esters. *J. Am. Chem. Soc.* **1973**, *95* (2), 512−519.
(46) Yamada, T.; Nomura, K.; Fujiki, M. Noticeable Chiral Center Dependence of Signs and Magnitudes in Circular Dichroism (CD) and Circularly Polarized Luminescence (CPL) Spectra of All Trans Poly(9,9 Dialkylfluorene 2,7 Vinylene)s Bearing Chiral Alkyl Side Chains in Solution, Aggregates, and Thin Films. *Macromolecules* **2018**, *51* (6), 2377−2387.
(47) Wei, X.; Tanaka, T.; Hirakawa, T.; Yomogida, Y.; Kataura, H. Determination of Enantiomeric Purity of Single Wall Carbon Nano tubes Using Flavin Mononucleotide. *J. Am. Chem. Soc.* **2017**, *139* (45), 16068−16071.
(48) Moss, G. P. Basic Terminology of Stereochemistry (IUPAC Recommendations 1996). *Pure Appl. Chem.* **1996**, *68* (12), 2193−2222.
(49) Peng, X.; Komatsu, N.; Kimura, T.; Osuka, A. Improved Optical Enrichment of SWNTs through Extraction with Chiral Nanotweezers of 2,6 Pyridylene Bridged Diporphyrins. *J. Am. Chem. Soc.* **2007**, *129* (51), 15947−15953.
(50) Chuang, K. C.; Nish, A.; Hwang, J. Y.; Evans, G. W.; Nicholas, R. J. Experimental Study of Coulomb Corrections and Single Particle Energies for Single Walled Carbon Nanotubes Using Cross Polarized Photoluminescence. *Phys. Rev. B: Condens. Matter Mater. Phys.* **2008**, *78* (8), 085411.
(51) Sato, N.; Tatsumi, Y.; Saito, R. Circular Dichroism of Single Wall Carbon Nanotubes. *Phys. Rev. B: Condens. Matter Mater. Phys.* **2017**, *95* (15), 155436.
(52) Wang, F.; Matsuda, K.; Rahman, A. F. M. M.; Peng, X.; Kimura, T.; Komatsu, N. Simultaneous Discrimination of Handedness and Diameter of Single Walled Carbon Nanotubes (SWNTs) with Chiral Diporphyrin Nanotweezers Leading to Enrichment of a Single Enantiomer of (6,5) SWNTs. *J. Am. Chem. Soc.* **2010**, *132* (31), 10876−10881.
(53) Berton, N.; Lemasson, F.; Poschlad, A.; Meded, V.; Tristram, F.; Wenzel, W.; Hennrich, F.; Kappes, M. M.; Mayor, M. Selective Dispersion of Large Diameter Semiconducting Single Walled Carbon Nanotubes with Pyridine Containing Copolymers. *Small* **2014**, *10* (2), 360−367.
(54) Humphrey, W.; Dalke, A.; Schulten, K. VMD: Visual Molecular Dynamics. *J. Mol. Graphics* **1996**, *14* (1), 33−38.
(55) Becke, A. D. A New Mixing of Hartree Fock and Local Density Functional Theories. *J. Chem. Phys.* **1993**, *98* (2), 1372−1377.
(56) Becke, A. D. Density Functional Thermochemistry. III. The Role of Exact Exchange. *J. Chem. Phys.* **1993**, *98* (7), 5648−5652.
(57) Weigend, F.; Ahlrichs, R. Balanced Basis Sets of Split Valence, Triple Zeta Valence and Quadruple Zeta Valence Quality for H to Rn: Design and Assessment of Accuracy. *Phys. Chem. Chem. Phys.* **2005**, *7* (18), 3297−3305.
(58) Zheng, J.; Xu, X.; Truhlar, D. G. Minimally Augmented Karlsruhe Basis Sets. *Theor. Chem. Acc.* **2011**, *128* (3), 295−305.
(59) Ahlrichs, R.; Furche, F.; Hättig, C.; Klopper, W. M.; Sierka, M.; Weigend, F. *TURBOMOLE*, Version 7.4; a development of University of Karlsruhe and Forschungszentrum Karlsruhe GmbH, 1989−2007; TURBOMOLE GmbH: Karlsruhe, 2019; available from http://www.turbomole.com.
(60) Case, D. A.; Belfon, K.; Ben Shalom, I. Y.; Brozell, S. R.; Cerutti, D. S.; Cheatham, T. E., III; Cruzeiro, V. W. D.; Darden, T. A.; Duke, R. E.; Giambasu, G.; Gilson, M. K.; Gohlke, H.; Goetz, A. W.; Harris, R.; Izadi, S.; Izmailov, S. A.; Kasavajhala, K.; Kovalenko, A.; Krasny, R.; Kurtzman, T.; et al. *Amber 2020*; University of California: San Francisco, 2020.

(61) Strunk, T.; Wolf, M.; Brieg, M.; Klenin, K.; Biewer, A.; Tristram, F.; Ernst, M.; Kleine, P. J.; Heilmann, N.; Kondov, I.; Wenzel, W. SIMONA 1.0: An Efficient and Versatile Framework for Stochastic Simulations of Molecular and Nanoscale Systems. *J. Comput. Chem.* **2012**, *33* (32), 2602−2613.
(62) Martínez, L.; Andrade, R.; Birgin, E. G.; Martínez, J. M. PACKMOL: A Package for Building Initial Configurations for Molecular Dynamics Simulations. *J. Comput. Chem.* **2009**, *30* (13), 2157−2164.
(63) Plimpton, S. Fast Parallel Algorithms for Short Range Molecular Dynamics. *J. Comput. Phys.* **1995**, *117* (1), 1−19.
(64) Sun, H. COMPASS: An *ab Initio* Force Field Optimized for Condensed Phase Applications−Overview with Details on Alkane and Benzene Compounds. *J. Phys. Chem. B* **1998**, *102* (38), 7338−7364.
(65) Sun, H.; Jin, Z.; Yang, C.; Akkermans, R. L. C.; Robertson, S. H.; Spenley, N. A.; Miller, S.; Todd, S. M. COMPASS II: Extended Coverage for Polymer and Drug Like Molecule Databases. *J. Mol. Model.* **2016**, *22*, 47.
(66) Deserno, M.; Holm, C. How to Mesh up Ewald Sums. II. An Accurate Error Estimate for the Particle−Particle−Particle Mesh Algorithm. *J. Chem. Phys.* **1998**, *109* (18), 7694−7701.